One-Pot Synthesis of High Surface Area Nano-Akaganeite Powder and Its Cation Sorption Behavior

Mamata Mohapatra,* Lagnamayee Mohapatra, Shashi Anand, and Barada Kanta Mishra

Institute of Minerals and Materials Technology, Bhubaneswar 751 013, Orissa, India

A one-pot novel facile synthesis of a high surface area nanoakaganeite (β-FeOOH) involving formation of a chelate as the precursor has been described. Ferric chloride solution mixed with ethylenediaminetetraacetic acid (EDTA) solution was heated to 90 °C followed by neutralization with ammonia to obtain a pH of 9, and the precipitate was stirred for half an hour. The precipitate was filtered, washed, and dried at 90 °C. Chemical, X-ray diffraction (XRD), Fourier transform infrared (FTIR), and Raman analyses confirmed the sample to be akaganeite. Transmission electron microscopy (TEM) studies showed the formation of monophase cigar-shaped akaganeite nanorods of (15 to 20) nm in width and (80 to 100) nm in length. The surface area obtained by the Brunauer−Emmett−Teller (BET) method was 176.16 $m^2 \cdot g^{-1}$. The nanopowder so obtained was used to generate sorption data for the removal of Pb(II), Cd(II), Cu(II), and Co(II) from aqueous solutions. The relative importance of experimental parameters such as solution pH, contact time, temperature, and concentration of adsorbate on the uptake of various cations was evaluated. The sorption kinetics followed a pseudosecond-order model. Both Langmuir and Freundlich models fitted the isothermic data of all of the cations well. High Langmuir monolayer capacities of (~163.9, 70.4, 80, and 98) $mg \cdot g^{-1}$ were obtained for Pb(II), Cd(II), Co(II), and Cu(II), respectively. The XRD patterns of Pb(II)-, Co(II)-, and Cu(II)-loaded samples showed positive shifts in *d*-values for the three main planes, that is, (110), (200), and (311) of akaganeite, while Cd(II)-loaded sample showed a negative shift in *d*-values of the (110) and (400) planes, indicating a disturbance in the internal structure during sorption.

Introduction

Akaganeite [β-FeO(OH)] is an important oxyhydroxide of iron that finds applications in many fields because of its unique sorption, ion-exchange, and catalytic properties.[1] Akaganeite with a tunnel structure is a promising catalytic material in chemical reactions. A band gap of 2.12 eV makes akaganeite a semiconductor.[2,3] This property makes it suitable for catalyzing oxidation or reduction reactions. β-FeOOH is also used as a precursor to prepare other iron compounds with special morphologies. Peng et al.[4] reported that single-crystal magnetite nanorods could be formed by hydrothermal reduction of β-FeOOH nanorods. Another very important application of akaganeite is as an adsorbent for water purification. Studies have been reported for the removal of cadmium, arsenic, and hexavalent chromium from aqueous solutions using akaganeite.[5−9] Generally $FeCl_3$ is hydrolyzed to synthesize akaganeite. The iron chloride solution needs to be heated to (70 to 100) °C for hydrolysis to occur, and the reaction time ranges from several hours to a few days. Yuan et al.[10] have reported for the first time the synthesis of mesoporous iron (oxyhydr)oxides with the crystalline phase of akaganeite by surfactant-mediated nanoparticle assembly. In the present study we have developed a one-pot synthesis method to obtain high surface area, pure monophasic nanosized akaganeite through a chelation-mediated technique, thereby reducing the preparation time to 1 h. The chelating agent used was ethylenediaminetetraacetic acid (EDTA), and ammonia was used as a precipitating agent. The high surface area coupled with the tunnel structure of akaganeite can make it an excellent adsorbent for toxic ion removal. With this view in mind the sorption properties of synthesized pure akaganeite were tested for Pb(II), Cd(II), Cu(II), and Co(II).

* Corresponding author. E-mail: mamatamohapatra@yahoo.com. Telephone: +91-674-2581126, ext. 272. Fax: +91-674-2581160.

Experimental Section

Chemicals. Ferric chloride hexahydrate ($FeCl_3 \cdot 6H_2O$; 99 %), NH_3, and EDTA were of analytical grade from Merck, India. Nitrate salts (Merck, India) of Pb(II), Co(II), Cu(II), and Cd(II) were used to prepare stock solutions for carrying out sorption studies.

Sample Preparation. A portion of 100 mL of 1 M solution of $FeCl_3 \cdot 6H_2O$ was mixed with 50 mL of 0.2 M EDTA solution in a three-necked Pyrex flask (500 mL) fitted with a condenser and a thermometer or pH electrode. The contents were heated to 363 K on a ceramic hot plate, followed by dropwise addition of 10 M ammonia (through one of the openings of the three-necked flask) until a pH of 9 was obtained. After precipitation the contents were stirred for half an hour, and the solution was air-cooled to room temperature. The suspension was filtered, washed until free of chloride, and then dried at a temperature of 90 °C. Two more samples were prepared (i) at room temperature without the addition of EDTA and (ii) at room temperature with the addition of EDTA.

Analysis and Characterization. The samples were acid-digested, and the iron was volumetrically analyzed.[11] The pH_{PZC} of the synthetic materials were determined following the Balistrieri and Murray method.[12] The crystal structures of the resulting products were characterized by X-ray diffraction (XRD; PW1830 XRD with Co Kα radiation with $\lambda = 1.79$ Å). The Fourier transform infrared (FTIR) spectra were taken using a JASCO model 5300 spectrometer in a KBr matrix in the range of (400 to 4000) cm^{-1}. A Raman spectrum was taken using a Renishaw (Renishaw plc, Gloucestershire, UK) in Via micro Raman spectrometer equipped with a 514 nm green laser having

10.1021/je9005932
Published on Web 03/04/2010

Table 1. Preparation Conditions (pH 9) and Chemical Analysis of Various Samples

sample no.	solutions	temp	% Fe	% chloride	pH_{PZC}
1	$FeCl_3 + NH_3$	ambient	53.44	0.54	5.43
2	$FeCl_3 + EDTA + NH_3$	ambient	58.93	5.79	5.83
3	$FeCl_3 + EDTA + NH_3$	90 °C	61.98	1.52	6.2

a 1 cm^{-1} spectral resolution of the Raman shift, a X−Y step resolution of 0.1 μm, and a confocal resolution of 2.5 μm. Surface area was measured with a Quantasorb 1750 instrument. The surface morphology of a typical sample was studied using electron microscopy (FEI, Tecnai G^2 20, Twin) operating at 200 kV, equipped with a Gatan charge-coupled device (CCD) camera. Samples for transmission electron microscopy (TEM) were prepared by first diluting a small amount of suspension with ethanol, sonicating, and placing a single drop of the resulting suspension onto a 200 mesh carbon-coated copper grid (SPI), which was then allowed to dry in air. Selected area electron diffraction (SAED) patterns were obtained with the smallest area aperture available (10 μm).

Sorption Experiments. The sorption experiments were carried out in an agitated horizontal shaker (160 rpm). The initial metal ion stock solutions were prepared from their respective nitrate salts. The pH of the initial metal ion solutions was adjusted, when needed, by addition of hydrochloric acid (0.1 N) or sodium hydroxide solution (0.01 M) and was measured with a Systronic micro pH instrument. For the sorption experiments, akaganeite concentrations of 2 $g \cdot L^{-1}$ were usually applied unless otherwise mentioned. In a typical experiment a weighed amount of sample was shaken with metal ion solution of required concentration for a predetermined contact time. After the sorption experiment, the suspension was filtered through a 0.45 μm membrane. The residual metal ions in the filtrate were analyzed after proper dilutions by a Perkin-Elmer atomic absorption spectrophotometer (Perkin-Elmer model AA200). To test the reproducibility, the experiments were carried out in triplicate, and the reproducibility was found to be within ± 2 %.

TCLP Test. A TCLP (toxicity characterization leaching procedure) test was used in this study that followed the standard procedures described by the USEPA.[13] About 1 g of sample was weighted into a polypropylene bottle. About 20 mL of the TCLP leachant (5.7 mL of CH_3COOH + 64.3 mL of 1 M NaOH at pH = 4.93) was added. The bottles were tumbled at 30 rpm in a horizontal shaker at room temperature for 20 h. At the end of the extraction, the leachate was filtered, and the leachate was acidified before being analyzed by atomic absorption spectroscopy (AAS).

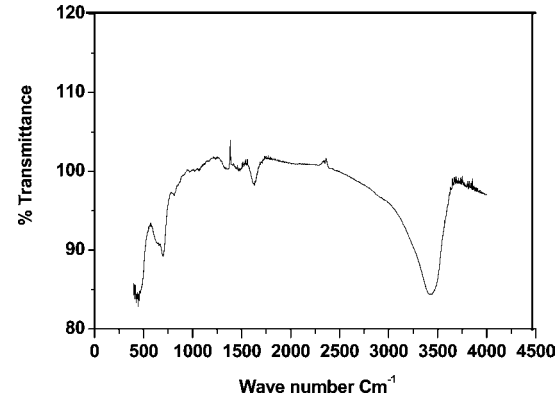

Figure 2. IR spectra of sample 3.

Results and Discussion

Chemical Analysis and Characterization of the Samples. All three samples were analyzed for both iron and chloride content. Preparation conditions for the three samples along with chemical analysis are given in Table 1. The samples have been coded as 1, 2, and 3. Figure 1 shows the XRD patterns of the products prepared at different experimental conditions. Sample 1 is totally amorphous in nature. Sample 2 is also amorphous in nature but shows the formation of a few broad peaks corresponding to the akaganeite phase. The XRD of sample 3 shows that all of the peaks are indexed to the tetragonal body-centered crystalline phase of β-FeO(OH) (akaganeite) with lattice constants b = 10.53 Å and c = 3.030 Å, which is in agreement with the literature values (JCPDS 34-1266). The intensity of the (211) peak was higher than that of the (310) peak, implying that the akaganeite was mainly present in the shape of rod-like crystals.[14] From the analysis and XRD patterns it is observed that only sample 3 shows well-defined crystalline monophase akaganeite. The chemical analysis showed this sample to contain 61.98 % iron. Because of the presence of a small percentage (1.54 %) of chloride, the iron content of the prepared akaganeite is somewhat lower than the theoretical value (62.9 %). Both chemical analysis as well as XRD analysis show that the presence of EDTA facilitates the nucleation of akaganeite under the present experimental conditions.

To confirm the absence of any other impurity, IR analysis was done. Figure 2 shows the IR spectra of akaganeite prepared at 90 °C in the presence of EDTA (sample 3). A wide band with a maximum at 3420 cm^{-1} is seen in the OH-stretching region, and a solitary band of H_2O-bending is located at 1630

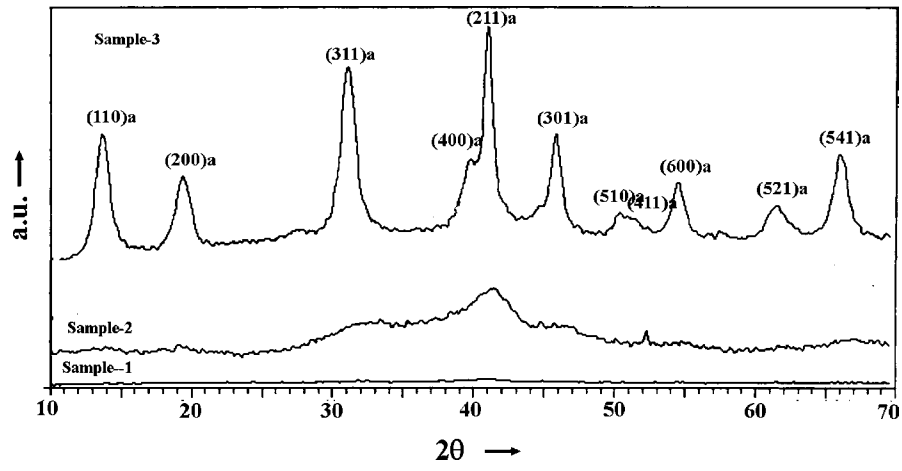

Figure 1. XRD patterns of various samples, a = akaganeite.

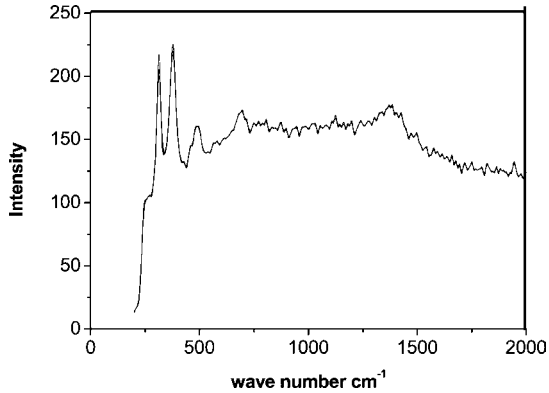

Figure 3. Raman spectra of sample 3.

cm^{-1}. The former might be related to the OH-stretching band(s) in akaganeite.[15] The absorption at 695.5 cm^{-1} is the characteristic vibration of Fe−O in β-FeOOH.[16,17] The band at 822 cm^{-1} is the libration modes of O−H−Cl hydrogen bonds present, which is characteristic of chloride-containing akaganeite.[17]

For further characterization, a Raman spectrum was taken (Figure 3). The band component analysis showed that two main peaks are identified at (310 and 380) cm^{-1}. Less intense bands are located at (490 and 700) cm^{-1}. These low-wavenumber regions correspond to the bands that are related to Fe−O stretching and Fe−OH bending vibrations for the akaganeite phase only.[18−20] The sharpness of the bands at (310 and 380) cm^{-1} is due to the low Cl content in the sample.[20] Lastly, a broad band is visible in the (1300 to 1450) cm^{-1} region which corresponds to the akaganeite phase.[21]

Figure 4a shows a typical TEM image of the as-synthesized β-FeOOH powder and reveals the formation of cigar-shaped particles with diameters of (15 to 20) nm and lengths of (80 to 100) nm. The nanoparticulate nature of the material is also evident from the broadness of the peaks in its powder XRD pattern as shown in Figure 1. The crystallite size in our samples is smaller than that of the akaganeite sample prepared by slow hydrolysis of $FeCl_3$ solution,[21] and the particles have a higher aspect ratio when compared to those prepared by Parfitt et al.[22] The high-resolution transmission electron image (HR-TEM) shows (Figure 4b) that the fringe spacing of 0.15 nm corresponds to the (200) plane, and the akaganeite grows along this plane. The corresponding selected area electron diffraction (SAED) pattern in Figure 4c shows that the reflections of the (110), (211), (411), (310), and (200) planes correspond to the akaganeite phase only.

The Brunauer−Emmett−Teller (BET) surface area of sample 3 was estimated to be 176.16 $m^2 \cdot g^{-1}$.

All of the above studies confirm sample 3 to be a monophasic nanoakaganeite having a high surface area. This sample was chosen to carry out sorption studies.

Possible Mechanism of the Formation of Akaganeite. The hydrolysis of Fe^{3+} from $FeCl_3$ solution proceeds as the reaction:

$$Fe^{3+} + 2H_2O \rightarrow FeO(OH) + 3H^+ \qquad (1)$$

to give the akaganeite (β-FeOOH) precipitates, normally under low pH. The tunnel structure of β-FeOOH often contains interstitial Cl^- anions. In the present work, the hydrolysis reaction of Fe(III) chloride in an EDTA−water solution at high pH is responsible for the formation of a nanostructured akaganeite phase. From the structural characteristics, EDTA plays a crucial role in the formation of octahedral crystals (a strong coordinating agent) by acting as a hexadentate ligand and wrapping itself around the metal ion with six suitable

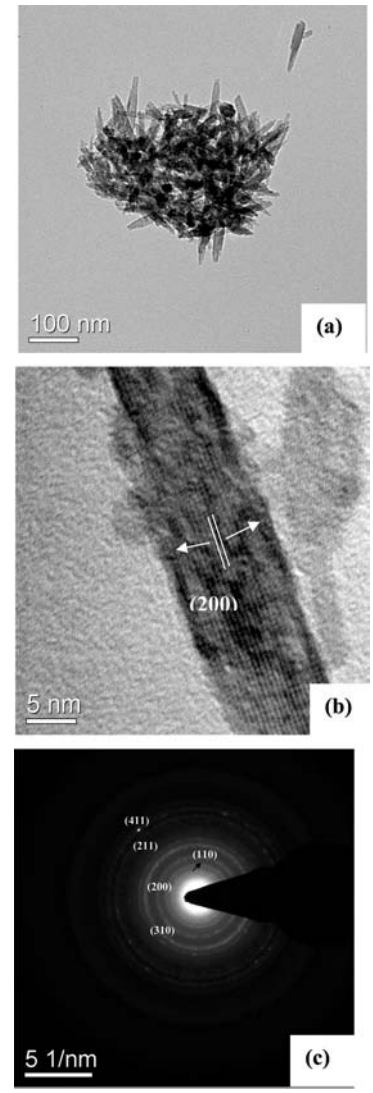

Figure 4. (a) TEM image, (b) high-resolution transmission electron image (HR-TEM), and (c) selected area diffraction (SAD) pattern of sample 3.

positions which can be gradually hydrated $[Fe(H_2O)_6]_2$ to β-FeOOH. The steric inhibition along the normal direction of the complex results in the preferential hydrolysis at the plane, and hence, the formation of β-FeOOH flakes with a (200) orientation. The precursor of $[Fe(EDTA)_3]^-$ seems to be vital for the formation of nano-rod alignment.

Sorption Kinetics. The sorption of Pb(II), Cd(II), Cu(II), and Co(II) on the synthesized akaganeite (sample 3) as a function of time was investigated (Figure 5) under the conditions of a sorbent concentration of 2 $g \cdot L^{-1}$, a sorbate concentration of 100 $mg \cdot L^{-1}$, pH 5, and a temperature of 308 K. Sorption of all metal ions achieved equilibrium in 1 h. All of the data were generated in triplicate, and the error bar is included in the same figure.

The time data up to 180 min was tested for kinetic models as given below:

Pseudofirst-order rate equation of Lagergren

$$\log(q_e - q_t) = \log q_e - k_1/2.303t \qquad (2)$$

Pseudosecond-order rate equation

$$t/q_t = 1/k_2 q_e^{\,2} + 1/q_e t \qquad (3)$$

where q_e and q_t are the amounts of the metal ions adsorbed ($mg \cdot g^{-1}$) at equilibrium and at time t (min), respectively. k_1 is

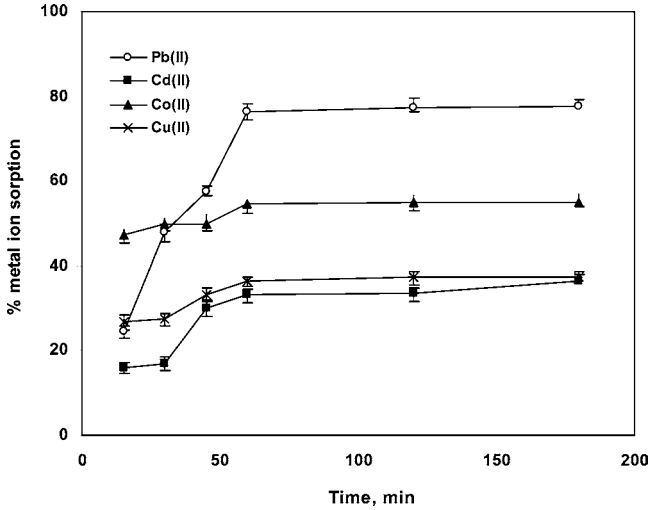

Figure 5. Effect of contact time on metal ion adsorption. Conditions: sorbent concentration of 2 g·L^{-1}, sorbate concentration of 100 mg·L^{-1}, pH 5, and temperature of 308 K.

Table 2. Kinetic Parameters for the Adsorption of Pb(II), Cd(II), Cu(II), and Co(II) on Akaganeite

	Pb(II)	Cd(II)	Cu(II)	Co(II)
q_{exp}	38.8	18.2	18.73	28.48
pseudofirst order				
$k_1 \cdot 10^{-2}$ (min^{-1})	5.89	2.00	4.22	4.33
q_e	68.45	10.78	12.46	7.51
r^2	0.92	0.71	0.96	0.83
pseudosecond order				
$k_2 \cdot 10^{-4}$ (g·mg^{-1}·min^{-1})	7.62	18.26	59.25	10.35
q_e	46.51	20.92	19.76	28.08
r^2	0.976	0.975	0.998	0.990

the sorption rate constant (min^{-1}) for first-order kinetics, and k_2 (g·mg^{-1}·min^{-1}) is the rate constant of the pseudosecond-order sorption reaction. The plots of (i) t/q_t versus t and (ii) log ($q_e - q_t$) versus t for the sorption of Pb(II), Cd(II), Cu(II), and Co(II) onto sample 3 (plots not shown) were used to get the rate parameters according to eqs 2 and 3.

The kinetic parameters for two kinetic models and coefficients of determination of four metal ions under similar conditions were calculated from these plots and are listed in Table 2. From this data it is observed that (i) pseudosecond-order reaction plots give r^2 values of > 0.97 for all metal ions and (ii) the experimental and theoretical q_e values match well suggesting the applicability of this kinetic model.

Effect of pH. The effect of pH on the removal of all four metal ions is depicted in Figure 6. The pH effect was studied up to a pH of 6 to avoid any precipitation combining with sorption. The experiments were run in triplicate. The variation in the results was within ± 2 %. It can be seen from Figure 6 that the sorption of metal ions increased with pH and reached a maximum at pH 5.25. With further increase of pH to 6, no significant increase in adsorption was observed. A similar pH effect has been observed by several authors that investigated metal sorption by different materials.[6,23−27] The increase in metal ion removal as the pH increases can be explained on the basis of a decrease in competition between proton and metal cations for the same functional groups and by a decrease in positive surface charge, which results in a lower electrostatic repulsion between the surface and the metal ions. The difference in sorption behavior of different heavy metal ions may be because of difference in their ion-exchange capacity on the surface depending on their charge density, extent of hydrolysis,

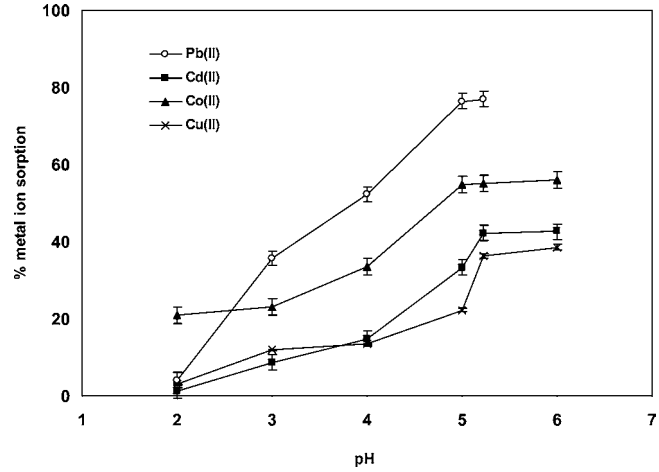

Figure 6. Effect of pH on metal ion sorption on sample 3. Conditions: metal ion concentration of 100 mg·L^{-1}, sorbent concentration of 2 g·L^{-1}, temperature of 308 K, and contact time of 1 h.

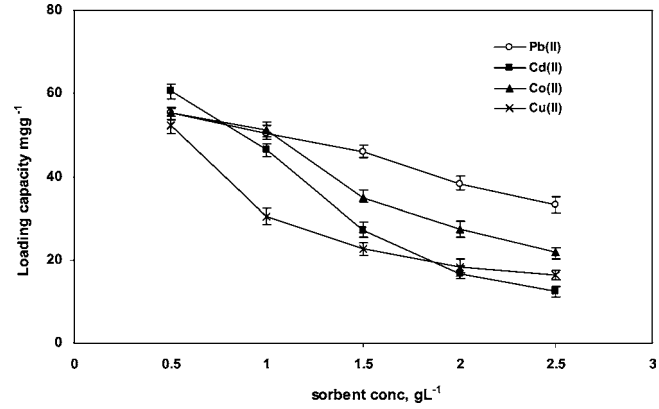

Figure 7. Effect of the sorbent dose on metal ion adsorption. Conditions: metal ion concentration of 100 mg·L^{-1}, pH 5, temperature of 308 K, and contact time of 1 h.

and solubility of hydrolyzed metal ions in solution under the present experimental conditions. It is often suggested that the sorption of metal ions at the solid−solution interface is not governed by free metal ions, but the much stronger adsorbed hydrolyzed metal species.[17]

Effect of Sorbent Dose. The dependence of metal ion sorption on the dose concentration was studied at different amounts of akaganeite varying from (0.5 to 2.5) g·L^{-1}. The initial pH was adjusted to 5. Figure 7 presents the loading capacities of each metal ion as a function of the sorbent concentration. The sorption capacities decreased from (55.3 to 33.24) mg·g^{-1}, (52.35 to 16.29) mg·g^{-1}, (60.5 to 12.35) mg·g^{-1}, and (55.5 to 21.97) mg·g^{-1} for Pb(II), Cu(II), Cd(II), and Co(II), respectively, by increasing the adsorbent dose from (0.5 to 2.5) g·L^{-1}. For the same initial metal ion concentration, the active sites increase because of the higher adsorbent dose, and hence the loading capacities decrease.

Effect of Concentration and Sorption Isotherms. The sorption isotherms were generated by varying the metal ion concentrations. A portion of 50 mL of metal ion solutions of different concentrations ranging from (50 to 600) mg·L^{-1} were contacted with 2 g·L^{-1} of adsorbent at a pH of 5.0, at 35 °C for a period of 1 h. Figure 8 shows plots of q_e versus C_e [where q_e has been defined earlier and C_e is the metal ion concentration (mg·L^{-1}) in solution at equilibrium].

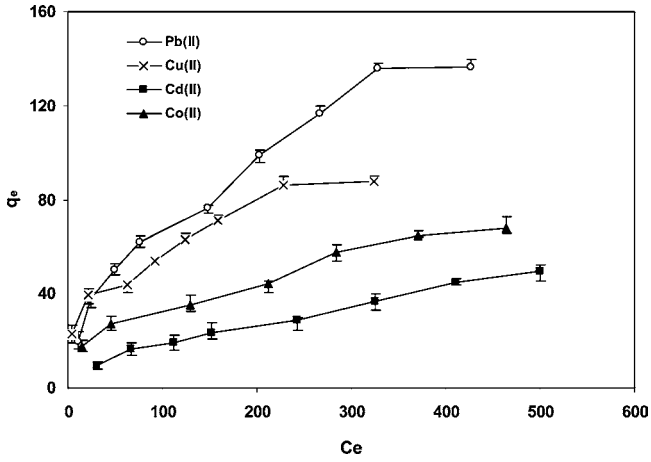

Figure 8. Adsorption isotherms showing q_e vs C_e. Conditions: sorbent concentration of 2 g·L^{-1}, pH 5, temperature of 308 K, and contact time of 1 h.

The well-known isotherm models are Langmuir and Freundlich, as given by eqs 4 and 5.

$$\text{Langmuir: } C_e/q_e = 1/(bq_m) + (1/q_m)C_e \quad (4)$$

where q_e and C_e have been defined earlier. q_m is the monolayer capacity.

$$\text{Freundlich: } q_e = K_F C_e^{1/n} \quad (5)$$

where K_F and $1/n$ are constants indicating the sorption capacity and the sorption intensity, respectively ($1/n < 1$). The Freundlich constant n indicates the degree of favorability of sorption.

Further, an essential feature of the Langmuir isotherm can be expressed in terms of a dimensionless constant separation factor or equilibrium parameter R_L,[22] given by eq 6.

$$\text{separation factor: } R_L = 1/(1 + bC_e) \quad (6)$$

For favorable adsorption R_L values should be < 1.[28]

The data of Figure 8 was fitted to the two models. The Langmuir and Freundlich sorption isotherms for all of the cations taken up for the present studies are shown in Figure 9a,b. The isothermic parameters are given in Table 3. Both of the models fit the isothermic data well. The Langmuir loading capacities have been estimated to be (163.9, 70.4, 80.0, and 98.0) mg·g^{-1} for Pb(II), Cd(II), Cu(II), and Co(II), respectively. The separation factors R_L with values of 0.39, 0.78, 0.57, and 0.33 for Pb(II), Cd(II), Co(II), and Cu(II), respectively, indicate favorable adsorption.[29] The data shows the highest K_F value for Cu(II) sorption (Table 3) and lowest K_F value for Cd(II) sorption, indicating the greatest binding of copper ion on akaganeite.

The high Langmuir monolayer capacities coupled with a short contact time and workable pH of 5 to 6 will make nano-akaganeite powder a potential good adsorbent for the removal of cations from contaminated water streams.

TCLP Study. TCLP tests were also carried out for the loaded samples. The limiting values set by the US Environmental Protection Agency (EPA, 1995),[13] are the following: 5 mg·L^{-1} for Pb and 1 mg·L^{-1} for Cd. During the test, the leachability of various cations was found to be 4.89 mg·L^{-1} for Pb(II), 0.75 mg·L^{-1} for Cd(II), 2.1 mg·L^{-1} for Cu(II), and 1.78 mg·L^{-1} for Co(II); hence, the loaded samples are stable.

XRD Study of Metal Ion Loaded Samples. The XRD patterns of the metal ion loaded samples are shown in Figure 10. From the XRD data, the shift in *d*-values were calculated taking the *d*-values of synthesized akaganeite sample 3 as base values. The

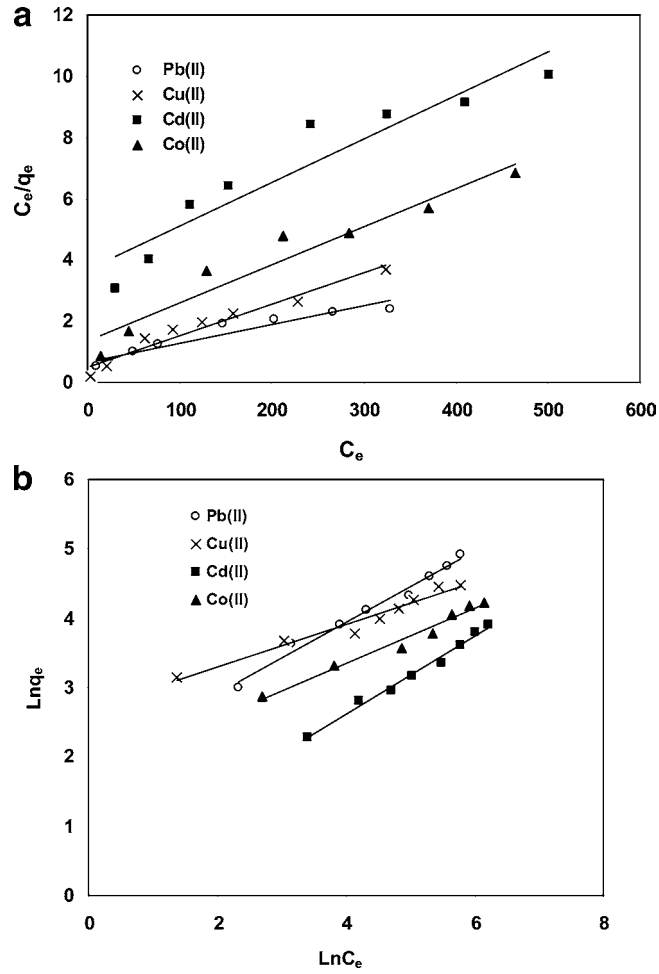

Figure 9. Adsorption isotherms. (a) Langmuir and (b) Freundlich. Data correspond to the average of those data given in Figure 8.

Table 3. Langmuir and Freundlich Parameters for the Adsorption of Cations on Sample 3

	Langmuir coefficients				Freundlich coefficients		
	q_m	b					
cations	mg·g^{-1}	L·g^{-1}	r^2	R_L	K_f	n	r^2
Pb(II)	163.9	0.009	0.925	0.39	6.595	1.95	0.985
Cd(II)	70.4	0.003	0.935	0.78	1.433	1.77	0.988
Co(II)	80.0	0.009	0.99	0.57	5.8979	2.54	0.976
Cu(II)	98.0	0.02	0.953	0.33	14.70	3.28	0.970

positive shifts in various planes of akaganeite after the adsorption of Pb(II), Co(II), and Cu(II) are given in Figure 11. It is observed that all three cations show maximum positive shifts for the (110), (200), and (311) planes, which confirms a

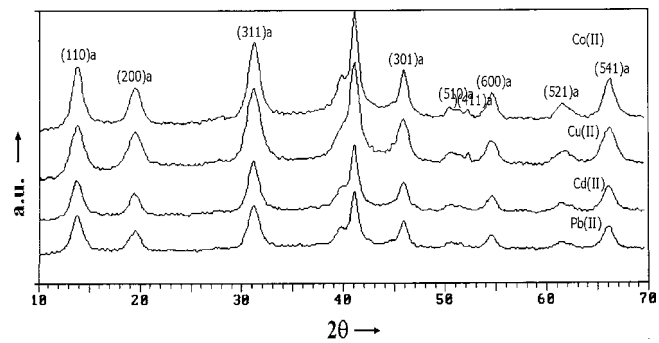

Figure 10. XRD of the metal ion loaded samples.

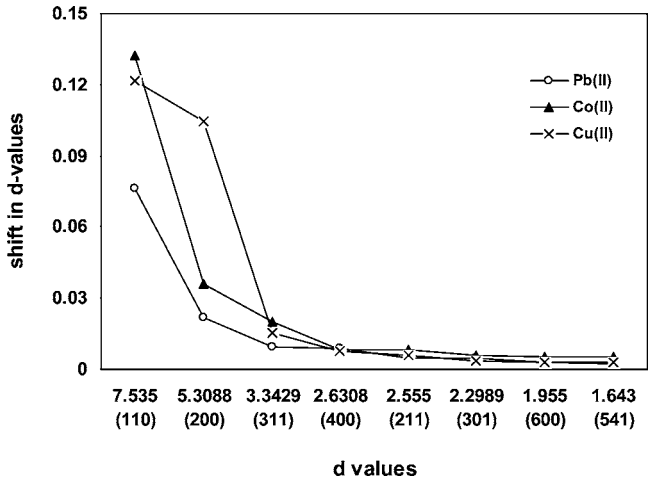

Figure 11. Positive shift of *d*-values of various planes (from XRD data of Figure 10) in metal ion loaded akaganeite samples.

disturbance in the crystal structure along these planes. Though there are positive shifts for other planes also, they are not very significant. In the case of Cd(II), negative shifts of 0.045 and 0.021 in *d*-values of planes (110) and (400), respectively, were observed. The shift is much less when compared to the other metal ions.

Conclusions

A high surface area (176.16 $m^2 \cdot g^{-1}$) nanoakaganeite (β-FeOOH) powder was synthesized using 1 M ferric chloride solution, 0.2 M EDTA solution as the chelating agent, and ammonia for neutralization. Chemical, XRD, FTIR, and Raman analyses confirmed the sample to be akaganeite. TEM studies showed the formation of monophase cigar-shaped akaganeite nanorods of (15 to 20) nm in width with (80 to 100) nm in length. The adsorption behavior of Pb(II), Cd(II), Cu(II), and Co(II) from aqueous solutions onto nanoakaganeite powder was studied. Various experimental parameters were varied to generate data including solution pH, contact time, temperature, and concentrations of adsorbate and adsorbent. With an increase in pH from 2 to 5, the uptake of metal ions increased. The sorption kinetics followed a pseudosecond-order model. Both the Langmuir and the Freundlich models fitted the isothermic data of all four cations well. High loading capacities of (~136, 50, 68, and 87.7) $mg \cdot g^{-1}$ were obtained for Pb(II), Cd(II), Co(II), and Cu(II), respectively. The XRD patterns of metal ion loaded samples, in general, showed positive shifts for different planes of akaganeite.

Acknowledgment

The authors are thankful to Prof. B. K. Mishra, Director, Institute of Minerals and Materials Technology, Bhubaneswar, for his kind permission to present this paper. The authors wish to thank Dr. R. K. Paramguru, Head Hydrometallurgy Department. The authors wish to thank to Dr. Biswarup Satpati and Dr. D. Behera for TEM and Raman analysis.

Literature Cited

(1) Mazeina, L.; Deore, S.; Navrotsky, A. Energetics of bulk and nanoakaganeite, β-FeOOH: enthalpy of formation, surface enthalpy, and enthalpy of water adsorption. *Chem. Mater.* **2006**, *18*, 1830–1838.
(2) Leland, J. K.; Bard, A. Photochemistry of collloidal semiconducting iron oxide polymorphs. *J. Phys. Chem.* **1987**, *91*, 5076–5083.
(3) White, A. F. *Reviews in Mineralogy 23*; Mineral Society of America: Washington, DC, 1990; p 447.
(4) Peng, Z. M.; Wu, M.; Xiong, Y.; Wang, J.; Chen, Q. Synthesis of magnetite nanorods through reduction of β-FeOOH. *Chem. Lett.* **2005**, *34*, 636–634.
(5) Deliyanni, E. A.; Bakoyannakis, D. N.; Zouboulis, A. I.; Matis, K. A. Sorption of As(V) ions by akaganeite-type nanocrystals. *Chemosphere* **2003**, *50*, 155–163.
(6) Deliyanni, E. A.; Matis, K. A. Sorption of Cd ions onto akaganeite-type nanocrystals. *Sep. Purif. Technol.* **2005**, *45*, 96–102.
(7) Music, S.; Krehula, S.; Popovic, S. Thermal decomposition of β-FeOOH. *Mater. Lett.* **2004**, *58*, 444–448.
(8) Music, S.; Krehula, S.; Popovic, S.; Skoko, Z. Some factors influencing forced hydrolysis of $FeCl_3$ solutions. *Mater. Lett.* **2003**, *57*, 1096–1102.
(9) Lazaridis, N. K.; Bakoyannakis, D. N.; Deliyanni, E. A. Chromium(VI) sorptive removal from aqueous solutions by nanocrystalline akaganeite. *Chemosphere* **2005**, *58*, 65–73.
(10) Yuan, Z. Y.; Ren, T. Z.; Su, B. L. Surfactant mediated nanoparticle assembly of catalytic mesoporous crystalline iron oxide materials. *Catal. Today* **2004**, *93*−*95*, 743–750.
(11) Vogel, A. I. *A Text Book of Quantitative Inorganic Analysis*; Longman Science and Technology: London, 2000.
(12) Balistrieri, L. S.; Murray, J. W. The adsorption of Cu, Pb, Zn, and Cd on goethite from major ion seawater. *Geochim. Cosmochim. Acta* **1982**, *46*, 1253–1265.
(13) *Test Methods for Evaluation of Solid Waste*, 3rd ed.; Laboratory Manual Physical/Chemical Methods SW86 40 CFR Parts 403 and 503; US EPA: Washington, DC, 1995.
(14) Cornell, R. M.; Schwetmann, U. *Iron Oxides in the Laboratory*; VCH Publishers: New York, 1991.
(15) Murad, E.; Bishop, J. L. The infrared spectrum of synthetic akaganéite, β-FeOOH. *Am. Mineral.* **2000**, *85*, 716–721.
(16) Schwertmann, U.; Murad, E. Effect of pH on the formation of goethite and hematite from ferrihydrite. *Clays Clay Miner.* **1983**, *31*, 277–284.
(17) Sugimoto, T.; Itoh, H.; Mochida, T. Shape control of monodisperse hematite particles by organic additives in the gel-sol system. *J. Colloid Interface Sci.* **1998**, *205*, 42–52.
(18) Nauer, G.; Strecha, P.; Brindakonopik, N.; Liptay, G. Spectroscopic and thermoanalytical characterization of standard substances for the identification of reaction products on iron electrodes. *J. Therm. Anal. Calorim.* **1985**, *30*, 813–830.
(19) Oh, S. J.; Cook, D. C.; Townsend, H. E. Characterization of iron oxides commonly formed as corrosion products on steel. *Hyperfine Interact.* **1998**, *112*, 59–65.
(20) Reguer, S.; Neff, D.; Ludovic, B. G.; Dillmann, P. Deterioration of iron archaeological artefacts: micro-Raman investigation on Cl-containing corrosion products. *J. Raman Spectrosc.* **2007**, *38*, 389–397.
(21) Cornell R. M.; Schwertmann, U. *The Iron Oxides*; Wiley-VCH: Weinheim, 2003.
(22) Parfitt, R. L.; Atkinson, R. J.; Smart, R. S. C. The mechanism of phosphate fixation by iron oxides. *Soil Sci. Soc. Am. Proc.* **1975**, *39*, 837–841.
(23) Kwon, J. S.; Yun, S. T.; Lee, J. H.; Kim, S. O.; Jo, H. Y. Removal of divalent heavy metals (Cd, Cu, Pb, and Zn) and arsenic (III) from aqueous solutions using scoria: Kinetics and equilibria of sorption. *J. Hazard. Mater.* **2010**, *174* (1−3), 307–313.
(24) Fiol, N.; Villaescusa, I.; Martínez, M.; Miralles, N.; Poch, J.; Serarols, J. Sorption of Pb(II), Ni(II), Cu(II) and Cd(II) from aqueous solution by olive stone waste. *Sep. Purif. Technol.* **2006**, *50* (1), 132–140.
(25) R Mohapatra, B. K.; Anand, S. Lead, cadmium and zinc adsorption on low grade manganese ore. *Int. J. Eng. Sci. Technol.* **2009**, *1* (1), 106–122.
(26) Mohapatra, M.; Rout, K.; Anand, S. Preparaion, characterization and heavy metal ion adsorption on Mg(II) doped goethite. *J. Hazard. Mater.* **2009**, *171* (1−3), 417–423.
(27) Mohapatra, M.; Khatun, S.; Anand, S. Kinetics and Thermodynamics of Lead (II) adsorption on Lateritic Nickel Ores of Indian Origin. *Chem. Eng. J.* **2009**, *155* (1−2), 184–190.
(28) Hall, K. R.; Eagleton, L. C.; Acrivos, A.; Vermeulen, T. Pore and solid diffusion kinetics in fixed bed adsorption under constant pattern conditions. *Ind. Eng. Chem. Fundam.* **1966**, *5*, 212–223.
(29) Sari, A.; Tuzen, M.; Citak, D.; Soylak, M. Equilibrium, kinetic and thermodynamic studies of adsorption of Pb(II) from aqueous solution onto Turkish kaolinite clay. *J. Hazard. Mater.* **2007**, *149*, 283–291.

Received for review July 14, 2009. Accepted February 12, 2010. The financial support provided by DST, India, under the Indo-Australia Strategic Research Scheme to carry out this work is thankfully acknowledged.

JE9005932